

# Synthesis, characterization and electrochemical performance of $\text{AlF}_3$ -coated $\text{Li}_{1.2}(\text{Mn}_{0.54}\text{Ni}_{0.16}\text{Co}_{0.08})\text{O}_2$ as cathode for Li-ion battery

Yan LI, Kai-yu LIU, Mei-yu LÜ, Lai WEI, Jian-jian ZHONG

School of Chemistry and Chemical Engineering, Central South University, Changsha 410083, China

Received 27 November 2013; accepted 12 May 2014

**Abstract:** Li-rich layered transitional metal oxide  $\text{Li}_{1.2}(\text{Mn}_{0.54}\text{Ni}_{0.16}\text{Co}_{0.08})\text{O}_2$  was prepared by sol–gel method and further modified by  $\text{AlF}_3$  coating via a wet process. The bare and  $\text{AlF}_3$ -coated  $\text{Li}_{1.2}(\text{Mn}_{0.54}\text{Ni}_{0.16}\text{Co}_{0.08})\text{O}_2$  samples were characterized by X-ray diffraction (XRD), scanning electron microscope (SEM), and high resolution transmission electron microscope (HRTEM). XRD results show that the bare and  $\text{AlF}_3$ -coated samples have typical hexagonal  $\alpha\text{-NaFeO}_2$  structure, and  $\text{AlF}_3$ -coated layer does not affect the crystal structure of the bare  $\text{Li}_{1.2}(\text{Mn}_{0.54}\text{Ni}_{0.16}\text{Co}_{0.08})\text{O}_2$ . Morphology measurements present that the  $\text{AlF}_3$  layer with a thickness of 5–7 nm is coated on the surface of the  $\text{Li}_{1.2}(\text{Mn}_{0.54}\text{Ni}_{0.16}\text{Co}_{0.08})\text{O}_2$  particles. Galvanostatic charge–discharge tests at various rates show that the  $\text{AlF}_3$ -coated  $\text{Li}_{1.2}(\text{Mn}_{0.54}\text{Ni}_{0.16}\text{Co}_{0.08})\text{O}_2$  has an enhanced electrochemical performance compared with the bare sample. At 1C rate, it delivers an initial discharge capacity of 208.2 mA·h/g and a capacity retention of 72.4% after 50 cycles, while those of the bare  $\text{Li}_{1.2}(\text{Mn}_{0.54}\text{Ni}_{0.16}\text{Co}_{0.08})\text{O}_2$  are 191.7 mA·h/g and 51.6 %, respectively.

**Key words:** lithium-ion battery;  $\text{Li}_{1.2}(\text{Mn}_{0.54}\text{Ni}_{0.16}\text{Co}_{0.08})\text{O}_2$ ;  $\text{AlF}_3$  surface coating; capacity retention

## 1 Introduction

In order to meet the requirement for electric vehicles (EVs) or hybrid electric vehicles (HEVs), lower cost, higher capacity and better safety are needed urgently for lithium-ion battery [1,2]. As one of the vital components of lithium-ion battery, cathode material largely determines the electrochemical performance of battery [3]. Recently, lithium-rich layered oxide  $\chi\text{Li}_2\text{MnO}_3 \cdot (1-\chi)\text{LiMO}_2$  ( $\text{M}=\text{Mn}, \text{Ni}, \text{Co}$ ) has drawn particular attention due to its high reversible capacity and good thermal stability [1], which are the most competitive features over conventional cathode materials, such as  $\text{LiCoO}_2$  and  $\text{LiMn}_2\text{O}_4$  for use in automotive applications. However, it suffers from some practical problems for commercial application, including poor rate capacity and bad cycling performance [4]. To overcome above drawbacks, surface coating is often used. Many inorganic compounds, such as metal oxides [5–7], fluorides [8–11] and phosphates [12], have been used to improve the electrochemical performance of cathode materials. Recently,  $\text{AlF}_3$  coating was reported to be a very effective way to improve the electrochemical

performance of  $\text{LiCoO}_2$  [13],  $\text{LiNi}_{0.5}\text{Mn}_{1.5}\text{O}_4$  [14],  $\text{Li}[\text{Ni}_{0.8}\text{Co}_{0.15}\text{Al}_{0.05}]\text{O}_2$  [15], etc. Generally, the improved electrochemical performance is attributed to the several reasons as follows: 1) the  $\text{AlF}_3$  layer can protect the electrode surface from HF attack in the electrolyte and suppress the dissolution of transition metal ions into the electrolyte, thereby reducing the charge transfer resistance [13,15]; 2) the coating layer can suppress the volume changes of electrode and thus prevent the cathode particles from being pulverized during cycling [15–17]. However, the exact role of  $\text{AlF}_3$  layer in Li-rich layered oxides is more complicated due to its special charge–discharge mechanism. By understanding the effect of  $\text{AlF}_3$  coating layer on the electrochemical performance of Li-rich layered oxides, the rate and cycling properties of Li-rich layered oxides can be improved effectively. Thus, it can be largely used in the electric vehicle field.

In this work,  $\text{AlF}_3$ -coated  $\text{Li}_{1.2}(\text{Mn}_{0.54}\text{Ni}_{0.16}\text{Co}_{0.08})\text{O}_2$  was prepared and characterized with respect to the bulk structure, surface state and electrochemical performance. Compared with the bare sample, the  $\text{AlF}_3$ -coated  $\text{Li}_{1.2}(\text{Mn}_{0.54}\text{Ni}_{0.16}\text{Co}_{0.08})\text{O}_2$  exhibits an obviously improved cycling performance and rate capacity. The

influence of the  $\text{AlF}_3$  coating on the Li-rich layered oxide is particularly addressed.

## 2 Experimental

### 2.1 Preparation and characterization

The Li-rich layered oxide,  $\text{Li}_{1.2}(\text{Mn}_{0.54}\text{Ni}_{0.16}\text{Co}_{0.08})\text{O}_2$ , was synthesized by sol-gel method, using citric acid (CA) and acetic salts as starting materials. Stoichiometric  $\text{Mn}(\text{CH}_3\text{COO})_2 \cdot 4\text{H}_2\text{O}$ ,  $\text{Ni}(\text{CH}_3\text{COO})_2 \cdot 4\text{H}_2\text{O}$ , and  $\text{Co}(\text{CH}_3\text{COO})_2 \cdot 4\text{H}_2\text{O}$  were dissolved in distilled water with 5% excess amount of  $\text{Li}(\text{CH}_3\text{COO}) \cdot \text{H}_2\text{O}$ . Then, the mixed solution was added dropwise to the citric acid solution with constant stirring. The solution pH was adjusted to 6 by using ammonium hydroxide. Subsequently, the solution was heated at 80 °C to obtain a dry solid. The resulting precursor was dried at 120 °C for 12 h and then calcined at 450 °C for 5 h to remove the organic impurities under air atmosphere. After being cooled to room temperature, the powder was pressed into pellets and sintered at 850 °C for 10 h to obtain the final product.

$\text{AlF}_3$ -coated  $\text{Li}_{1.2}(\text{Mn}_{0.54}\text{Ni}_{0.16}\text{Co}_{0.08})\text{O}_2$  was obtained through a wet coating process. The bare  $\text{Li}_{1.2}(\text{Mn}_{0.54}\text{Ni}_{0.16}\text{Co}_{0.08})\text{O}_2$  powders were immersed into  $\text{Al}(\text{NO}_3)_3$  aqueous solution. Then a  $\text{NH}_4\text{F}$  aqueous solution was added slowly, in which the molar ratio of Al to F was controlled to be 1:3. The mixed solution was stirred at 80 °C for 5 h, followed by drying at 60 °C in a vacuum oven. Finally, the mixture was sintered at 400 °C for 5 h under Ar atmosphere. The nominal amount of  $\text{AlF}_3$  was about 0.5% (volume fraction) of the parent material.

The crystalline structure of the samples was confirmed by X-ray diffraction (XRD, D/maxIII, Rigaku) with a range of  $2\theta$  from 10° to 90°. The morphology and composition of the samples were examined with a scanning electron microscope (SEM, Quanta-200) equipped with an energy-dispersive X-ray spectrometer (EDS, EDAX). The  $\text{AlF}_3$ -coated layer was investigated with a high resolution transmission electron microscope (HRTEM, JEOL-3010).

### 2.2 Electrochemical measurements

Coin-type (CR2016) half-cells were assembled to evaluate electrochemical properties of the prepared samples. Electrodes were prepared by casting the slurry, with the composition of active materials (80%), conducting agent (Super-P, 10%), and binder PVDF (polyvinylidene fluoride, 10%) onto Al foil. A porous polyethylene (PE) membrane was used as a separator and Li metal foil was used as counter and reference electrodes. The electrolyte was  $\text{LiPF}_6$  (1 mol/L) in a mixture of ethylene carbonate (EC) and dimethyl

carbonate (DMC) with a volume ratio of 3:7. Cells were cycled galvanostatically at different constant current rates ( $1\text{C}=200\text{ mA}\cdot\text{h/g}$ ) between 2.5 and 4.8 V (vs  $\text{Li/Li}^+$ ). Cyclic voltammograms for the samples were obtained in a voltage range of 2.0–4.8 V (vs  $\text{Li/Li}^+$ ) with a scan rate of 0.1 mV/s. Electrochemical impedance measurements were performed over a frequency range from 100 kHz to 0.01 Hz with the amplitude of 5 mV.

## 3 Results and discussion

### 3.1 Microstructure

Figure 1 shows the XRD patterns of the bare and  $\text{AlF}_3$ -coated  $\text{Li}_{1.2}(\text{Mn}_{0.54}\text{Ni}_{0.16}\text{Co}_{0.08})\text{O}_2$  samples. All the diffraction peaks of both samples could be indexed with hexagonal  $\alpha\text{-NaFeO}_2$  structure with a space group of  $R_3/m$  [18]. The clear separations between the adjacent peaks of (006)/(102) and (018)/(110) indicated an ordering structure of  $R_3/m$  single phase. The weak peaks at 20°–23° represented the monoclinic  $\text{Li}_2\text{MnO}_3$ -like component ( $C_2/m$ ) in the structure, caused by the short range ordering of the  $\text{Li}^+$ ,  $\text{Ni}^{2+}$  and  $\text{Mn}^{4+}$  in the transition metal layer [19]. Compared with the bare sample, no impurity peaks were observed from the  $\text{AlF}_3$ -coated  $\text{Li}_{1.2}(\text{Mn}_{0.54}\text{Ni}_{0.16}\text{Co}_{0.08})\text{O}_2$  patterns due to the amorphous and low content  $\text{AlF}_3$ . The lattice parameters of the bare and  $\text{AlF}_3$ -coated  $\text{Li}_{1.2}(\text{Mn}_{0.54}\text{Ni}_{0.16}\text{Co}_{0.08})\text{O}_2$  samples were calculated according to the hexagonal structure with  $R_3/m$  space group by using MDI Jade 5.0 software. The refined data of the bare sample were  $a=2.855\text{ Å}$ ,  $c=14.244\text{ Å}$ , and  $V=100.59\text{ Å}^3$ , with  $c/a$  ratio of 4.988. The values of  $\text{AlF}_3$ -coated  $\text{Li}_{1.2}(\text{Mn}_{0.54}\text{Ni}_{0.16}\text{Co}_{0.08})\text{O}_2$  were  $a=2.856\text{ Å}$ ,  $c=14.250\text{ Å}$ , and  $V=100.67\text{ Å}^3$ , with  $c/a$  ratio of 4.989. There was no significant difference between lattice parameters of the bare and  $\text{AlF}_3$ -coated samples, indicating that the  $\text{AlF}_3$  coating had little influence on the bulk structure of  $\text{Li}_{1.2}(\text{Mn}_{0.54}\text{Ni}_{0.16}\text{Co}_{0.08})\text{O}_2$ .

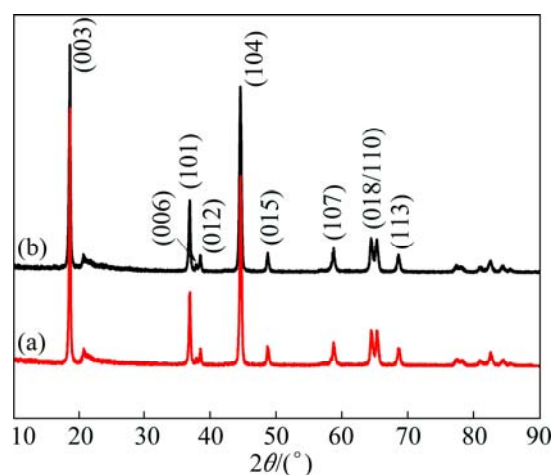


**Fig. 1** XRD patterns of bare  $\text{Li}_{1.2}(\text{Mn}_{0.54}\text{Ni}_{0.16}\text{Co}_{0.08})\text{O}_2$  (a) and  $\text{AlF}_3$ -coated  $\text{Li}_{1.2}(\text{Mn}_{0.54}\text{Ni}_{0.16}\text{Co}_{0.08})\text{O}_2$  (b)

SEM images of the bare and  $\text{AlF}_3$ -coated  $\text{Li}_{1.2}(\text{Mn}_{0.54}\text{Ni}_{0.16}\text{Co}_{0.08})\text{O}_2$  are presented in Fig. 2. It can be seen that both of the samples contained aggregates of primary, nano-sized particles. These primary particles were homogeneous and had a small size of 100–200 nm. There is no large difference between the bare and  $\text{AlF}_3$ -coated  $\text{Li}_{1.2}(\text{Mn}_{0.54}\text{Ni}_{0.16}\text{Co}_{0.08})\text{O}_2$  due to the nano-thickness of  $\text{AlF}_3$ -coated layer. More detailed morphology for  $\text{AlF}_3$ -coated  $\text{Li}_{1.2}(\text{Mn}_{0.54}\text{Ni}_{0.16}\text{Co}_{0.08})\text{O}_2$  was observed by HRTEM analysis in Fig. 3(a). Visibly, a  $\text{AlF}_3$  layer with a thickness of 5–7 nm appeared in the edge of the coated  $\text{Li}_{1.2}(\text{Mn}_{0.54}\text{Ni}_{0.16}\text{Co}_{0.08})\text{O}_2$ . Moreover, EDS analysis of the  $\text{AlF}_3$ -coated  $\text{Li}_{1.2}(\text{Mn}_{0.54}\text{Ni}_{0.16}\text{Co}_{0.08})\text{O}_2$  in Fig. 3(b) revealed the presence of Al and F besides Co, Ni and Mn on the surface of  $\text{AlF}_3$ -coated  $\text{Li}_{1.2}(\text{Mn}_{0.54}\text{Ni}_{0.16}\text{Co}_{0.08})\text{O}_2$ .

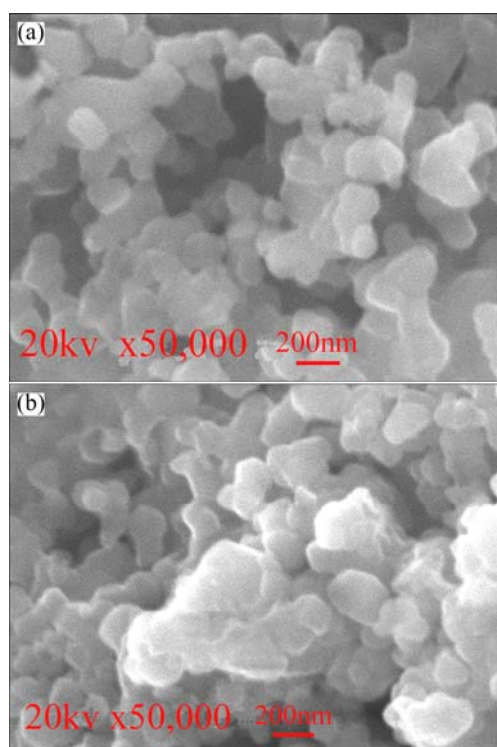


Fig. 2 SEM images of bare (a) and  $\text{AlF}_3$ -coated  $\text{Li}_{1.2}(\text{Mn}_{0.54}\text{Ni}_{0.16}\text{Co}_{0.08})\text{O}_2$  (b)

### 3.2 Galvanostatic charge–discharge characterization

Figure 4 shows the initial charge and discharge curves of the bare and  $\text{AlF}_3$ -coated  $\text{Li}_{1.2}(\text{Mn}_{0.54}\text{Ni}_{0.16}\text{Co}_{0.08})\text{O}_2$  electrodes at 0.1C in the voltage range of 2.5–4.8 V. Both samples exhibited two plateaus during the initial charge, due to the existence of two different lithium de-insertion processes. The first plateau located at 3.8–4.4 V was associated to the lithium removal from the layered component,  $\text{LiMO}_2$ , corresponding to the oxidation of  $\text{Ni}^{2+} \rightarrow \text{Ni}^{4+}$  and  $\text{Co}^{3+} \rightarrow \text{Co}^{4+}$ , and the discharge capacity was close to the theoretical capacity (120 mA·h/g). The second plateau, characterized by a relatively flat voltage profile above

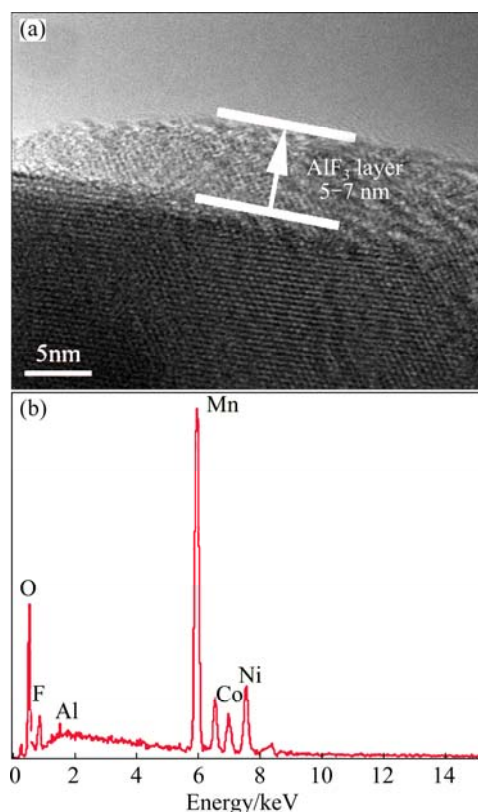


Fig. 3 HRTEM image (a) and EDS result (b) of  $\text{AlF}_3$ -coated  $\text{Li}_{1.2}(\text{Mn}_{0.54}\text{Ni}_{0.16}\text{Co}_{0.08})\text{O}_2$

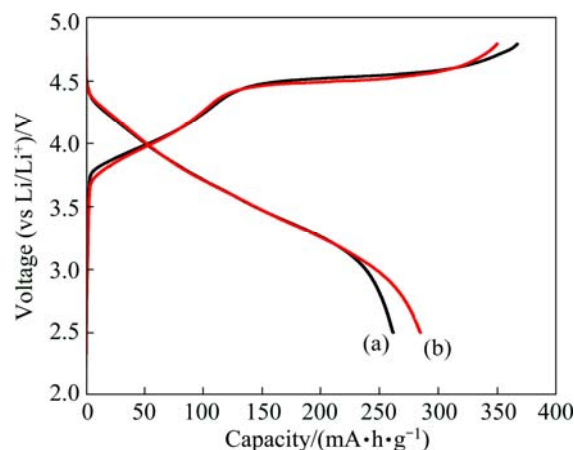
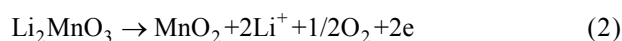


Fig. 4 Initial charge and discharge curves of bare  $\text{Li}_{1.2}(\text{Mn}_{0.54}\text{Ni}_{0.16}\text{Co}_{0.08})\text{O}_2$  (a) and  $\text{AlF}_3$ -coated  $\text{Li}_{1.2}(\text{Mn}_{0.54}\text{Ni}_{0.16}\text{Co}_{0.08})\text{O}_2$  (b) electrodes at 0.1C rate in voltage range of 2.5–4.8 V at room temperature

4.4 V, originated from the loss of oxygen from the layered  $\text{Li}_2\text{MnO}_3$  component, which might be transformed to an electrochemical active  $\text{MnO}_2$ -like phase [20,21]. The corresponding reactions could be represented as follows:



It could be observed that the initial discharge

capacities of the bare and  $\text{AlF}_3$ -coated  $\text{Li}_{1.2}(\text{Mn}_{0.54}\text{Ni}_{0.16}\text{Co}_{0.08})\text{O}_2$  were 261.3  $\text{mA}\cdot\text{h/g}$  and 284.5  $\text{mA}\cdot\text{h/g}$ , and the initial coulombic efficiencies of the samples increased from 71.18 % to 81.29 %.

Figure 5 shows the discharge profiles of the bare and  $\text{AlF}_3$ -coated  $\text{Li}_{1.2}(\text{Mn}_{0.54}\text{Ni}_{0.16}\text{Co}_{0.08})\text{O}_2$  electrodes at different rates (1/20C, 1/10C, 1/5C, 1C, 2C, 5C) between 2.5 and 4.8 V at room temperature. It can be seen that the discharge capacity of the  $\text{AlF}_3$ -coated  $\text{Li}_{1.2}(\text{Mn}_{0.54}\text{Ni}_{0.16}\text{Co}_{0.08})\text{O}_2$  electrode was slightly higher than that of the bare electrode. In detail, the initial discharge capacities of the bare  $\text{Li}_{1.2}(\text{Mn}_{0.54}\text{Ni}_{0.16}\text{Co}_{0.08})\text{O}_2$  at 1/20, 1/10 and 1/5, 1, 2 and 5C rates were 280.5, 261.3, 249.3, 191.7, 136.5 and 90.9  $\text{mA}\cdot\text{h/g}$ , respectively, while those of the  $\text{AlF}_3$ -coated  $\text{Li}_{1.2}(\text{Mn}_{0.54}\text{Ni}_{0.16}\text{Co}_{0.08})\text{O}_2$  were 296.8, 284.5, 266.9, 208, 166.9 and 110.3  $\text{mA}\cdot\text{h/g}$ , respectively. Due to the fact that the bare and  $\text{AlF}_3$ -coated  $\text{Li}_{1.2}(\text{Mn}_{0.54}\text{Ni}_{0.16}\text{Co}_{0.08})\text{O}_2$  were charged to high cutoff voltage of 4.8 V, where electrolyte decomposition became the main factor affecting their electrochemical performance, the electrolyte decomposition could lead to the formation of LiF-containing film on the electrodes, increasing the interface resistance and deteriorating the

electrochemical performance. However, the  $\text{AlF}_3$ -coated layer may reduce the formation of LiF film, and would thus suppress the cathode–electrolyte interfacial impedance.

Figure 6 presents the cycling performance of the bare and  $\text{AlF}_3$ -coated  $\text{Li}_{1.2}(\text{Mn}_{0.54}\text{Ni}_{0.16}\text{Co}_{0.08})\text{O}_2$  electrodes at 1C in the voltage range of 2.5–4.8 V. During the extended cycling, the bare  $\text{Li}_{1.2}(\text{Mn}_{0.54}\text{Ni}_{0.16}\text{Co}_{0.08})\text{O}_2$  electrode exhibited a rapid capacity loss, leading to a capacity retention of only 51.6% after 50 cycles. This poor performance was ascribed to the transition metal dissolution of the electrode surface resulting from HF attack, which causes severe serration of electrode particle surface [22]. However, the  $\text{AlF}_3$ -coated  $\text{Li}_{1.2}(\text{Mn}_{0.54}\text{Ni}_{0.16}\text{Co}_{0.08})\text{O}_2$  electrode demonstrated a greatly improved cycling performance, exhibiting a capacity retention of 72.4% due to the encapsulation of particle surface of  $\text{AlF}_3$  layer. And it is worth noticing that the capacity of the  $\text{AlF}_3$ -coated  $\text{Li}_{1.2}(\text{Mn}_{0.54}\text{Ni}_{0.16}\text{Co}_{0.08})\text{O}_2$  electrode increased during 1–8 cycles before decreasing. This phenomenon could be explained as follows. It is a mandatory process for  $\chi\text{Li}_2\text{MnO}_3\cdot(1-\chi)\text{LiMO}_2$  to be charged above 4.6 V (vs Li/Li<sup>+</sup>) to deliver large discharge capacity more than 200  $\text{mA}\cdot\text{h/g}$  [23]. In the high potential region, the oxygen release as  $\text{Li}_2\text{O}$  from the lattice is unavoidable, accompanied with the generation of oxygen vacancies through ionic rearrangements at the end of the initial charge. The polarization in the high potential region is lower for the  $\text{AlF}_3$ -coated  $\text{Li}_{1.2}(\text{Mn}_{0.54}\text{Ni}_{0.16}\text{Co}_{0.08})\text{O}_2$ , resulting in the effective lithium extraction and subsequent insertion. In other words, the existence of the  $\text{AlF}_3$ -coated layer can retain more oxygen vacancies generated in the initial charge process, which is responsible for more lithium-ion insertion and the capacity increase during the subsequent discharge process.

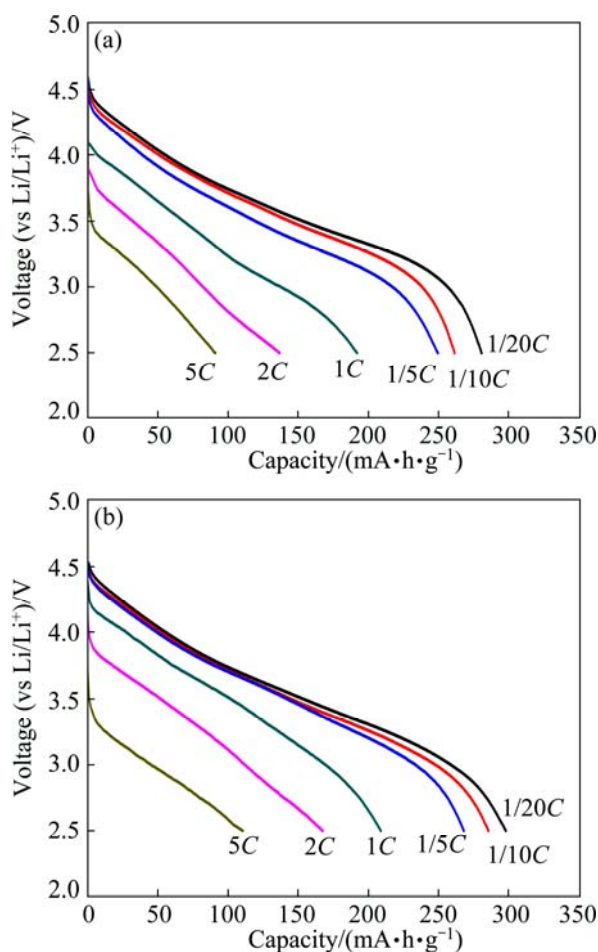


**Fig. 5** Discharge curves of bare (a) and  $\text{AlF}_3$ -coated  $\text{Li}_{1.2}(\text{Mn}_{0.54}\text{Ni}_{0.16}\text{Co}_{0.08})\text{O}_2$  (b) electrodes cycled at different rates in voltage range of 2.5–4.8 V at room temperature

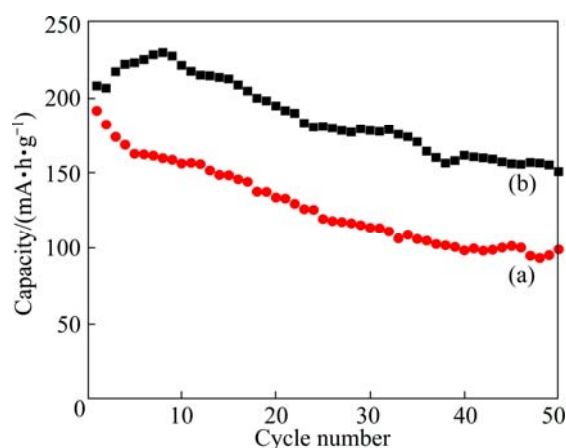


**Fig. 6** Cycling performance of bare (a) and  $\text{AlF}_3$ -coated  $\text{Li}_{1.2}(\text{Mn}_{0.54}\text{Ni}_{0.16}\text{Co}_{0.08})\text{O}_2$  (b) electrodes at 1C in voltage range of 2.5–4.8 V



### 3.3 Cyclic voltammetric (CV) analysis

To explore the improved electrochemical performance of  $\text{AlF}_3$ -coated  $\text{Li}_{1.2}(\text{Mn}_{0.54}\text{Ni}_{0.16}\text{Co}_{0.08})\text{O}_2$ , cyclic voltammetry tests were performed to compare the electrochemical reaction kinetics of the bare and  $\text{AlF}_3$ -coated  $\text{Li}_{1.2}(\text{Mn}_{0.54}\text{Ni}_{0.16}\text{Co}_{0.08})\text{O}_2$ . Figure 7 displays the CV curves (initial and the second cycle) of the bare and  $\text{AlF}_3$ -coated  $\text{Li}_{1.2}(\text{Mn}_{0.54}\text{Ni}_{0.16}\text{Co}_{0.08})\text{O}_2$  at 0.1 mV/s in the voltage range of 2.0–4.8 V (vs  $\text{Li}/\text{Li}^+$ ). Both of the samples showed the characteristic CV curves of the  $\chi\text{Li}_2\text{MnO}_3 \cdot (1-\chi)\text{LiMO}_2$  type materials, which had a large oxidation peak around 4.6 V [24]. The peak was the result from irreversible removal of  $\text{Li}_2\text{O}$  from the  $\text{Li}_2\text{MnO}_3$  component and the formation of an electrochemically active  $\text{MnO}_2$  component. The disappearance of the peak during the second cycle confirmed its irreversibility. The redox around 3.0 V could provide the proof for the formation of  $\text{MnO}_2$ . It has been reported that  $\text{MnO}_2$  had electrochemical reactivity with lithium in the voltage between 2.0 and 3.0 V [25]. As shown in Fig. 8, the couple was clearly observed for the  $\text{AlF}_3$ -coated  $\text{Li}_{1.2}(\text{Mn}_{0.54}\text{Ni}_{0.16}\text{Co}_{0.08})\text{O}_2$ , but it was weak for the bare one. The redox peaks of  $\text{Mn}^{3+}/\text{Mn}^{4+}$  are higher and broader in  $\text{AlF}_3$ -coated  $\text{Li}_{1.2}(\text{Mn}_{0.54}\text{Ni}_{0.16}\text{Co}_{0.08})\text{O}_2$

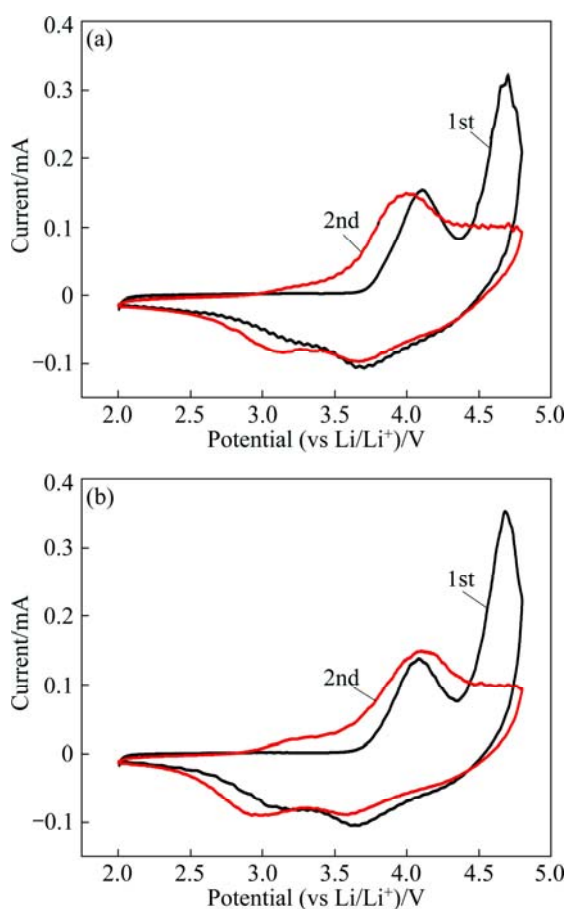


**Fig. 7** Cyclic voltammetry curves of bare (a) and  $\text{AlF}_3$ -coated  $\text{Li}_{1.2}(\text{Mn}_{0.54}\text{Ni}_{0.16}\text{Co}_{0.08})\text{O}_2$  (b) at scan rate of 0.1 mV/s in voltage range of 2.0–4.8 V (vs  $\text{Li}/\text{Li}^+$ )

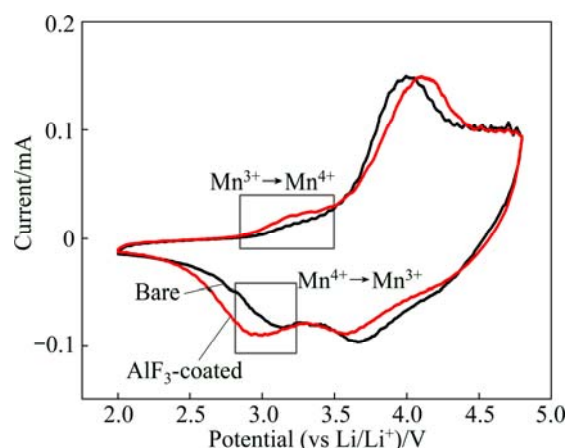


**Fig. 8** Comparison of bare and  $\text{AlF}_3$ -coated  $\text{Li}_{1.2}(\text{Mn}_{0.54}\text{Ni}_{0.16}\text{Co}_{0.08})\text{O}_2$  at the second cyclic voltammetry

$\text{Co}_{0.08})\text{O}_2$  than in the bare electrode. The results implied that the pre-active  $\text{MnO}_2$  of the  $\text{AlF}_3$ -coated  $\text{Li}_{1.2}(\text{Mn}_{0.54}\text{Ni}_{0.16}\text{Co}_{0.08})\text{O}_2$  sample was better than the bare one. Thus, the  $\text{AlF}_3$ -coated  $\text{Li}_{1.2}(\text{Mn}_{0.54}\text{Ni}_{0.16}\text{Co}_{0.08})\text{O}_2$  electrode exhibited better performance than the bare one.

### 3.4 Electrochemical impedance spectroscopic analysis

To correlate the electrochemical performance with interfacial impedance, electrochemical impedance spectroscopy was performed for the bare and  $\text{AlF}_3$ -coated  $\text{Li}_{1.2}(\text{Mn}_{0.54}\text{Ni}_{0.16}\text{Co}_{0.08})\text{O}_2$  electrodes. Both of the electrodes were tested after 30 charge–discharge cycles at 0.1C rate. Nyquist plots of the two electrodes are compared in Fig. 9. The plots of both electrodes consisted of two semicircles, one in the high to medium frequency region, the other in the medium to low frequency region and a straight line in the low-frequency region. The semicircle in the high to medium frequency region was related to the surface film resistance ( $R_{\text{sf}}$ ); the semicircle in the medium to low frequency resulted from the charge transfer resistance ( $R_{\text{ct}}$ ); the straight line in the

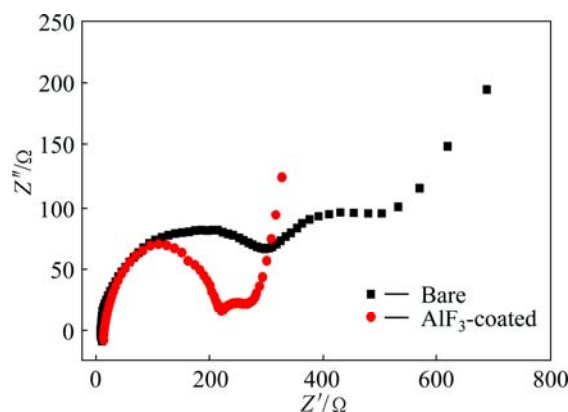


**Fig. 9** Electrochemical impedance spectra (EIS) of bare and  $\text{AlF}_3$ -coated  $\text{Li}_{1.2}(\text{Mn}_{0.54}\text{Ni}_{0.16}\text{Co}_{0.08})\text{O}_2$  electrodes

low-frequency region corresponded to a semi-infinite Warburg diffusion process (solid state diffusion of lithium ions through the bulk of the electrode) [26]. In Fig. 9, it is shown that the total resistance of the bare electrode was much larger than that of  $\text{AlF}_3$ -coated one. Especially, the charge-transfer resistance was notably reduced after  $\text{AlF}_3$  coating. It seemed that the  $\text{AlF}_3$ -coated layer on the surface of  $\text{Li}_{1.2}(\text{Mn}_{0.54}\text{Ni}_{0.16}\text{Co}_{0.08})\text{O}_2$  could lower the activity of interface between electrode and electrolyte, facilitating lithium-ion conduction by reducing charge-transfer resistance. Then, the better lithium-ion conduction would improve the cycling performance of  $\text{AlF}_3$ -coated  $\text{Li}_{1.2}(\text{Mn}_{0.54}\text{Ni}_{0.16}\text{Co}_{0.08})\text{O}_2$  electrodes as described in Fig. 6.

## 4 Conclusions

1) Uniform and thin  $\text{AlF}_3$  layer with a thickness of 5–7 nm is coated on the surface of  $\text{Li}_{1.2}(\text{Mn}_{0.54}\text{Ni}_{0.16}\text{Co}_{0.08})\text{O}_2$  particles by a wet process.

2) The  $\text{AlF}_3$ -coated  $\text{Li}_{1.2}(\text{Mn}_{0.54}\text{Ni}_{0.16}\text{Co}_{0.08})\text{O}_2$  has better electrochemical performance than the bare  $\text{Li}_{1.2}(\text{Mn}_{0.54}\text{Ni}_{0.16}\text{Co}_{0.08})\text{O}_2$ . At 0.1C rate, the initial coulombic efficiency of the  $\text{Li}_{1.2}(\text{Mn}_{0.54}\text{Ni}_{0.16}\text{Co}_{0.08})\text{O}_2$  is improved from 71.18 % to 81.29 % by  $\text{AlF}_3$  coating. And the capacity retention is improved from 51.6% to 72.4 % after 50 cycles at 1C rate.

3) EIS results show that the improved electrochemical performance of  $\text{AlF}_3$ -coated  $\text{Li}_{1.2}(\text{Mn}_{0.54}\text{Ni}_{0.16}\text{Co}_{0.08})\text{O}_2$  can be explained by the lower charge transfer resistance. CV tests also indicate the better pre-active of  $\text{MnO}_2$  by  $\text{AlF}_3$  coating.

## References

- [1] HU Meng, PANG Xiao-li, ZHOU Zhen. Recent progress in high-voltage lithium ion batteries [J]. *Journal of Power Sources*, 2013, 237: 229–242.
- [2] PATIL A, PATIL V, WOOK S D, CHOI J W, PAIK D S, YOON S J. Issue and challenges facing rechargeable thin film lithium batteries [J]. *Materials Research Bulletin*, 2008, 43(8–9): 1913–1942.
- [3] XU Bo, QIAN Dan-na, WANG Zi-ying, MENG Ying-shirley. Recent progress in cathode materials research for advanced lithium ion batteries [J]. *Materials Science and Engineering R*, 2012, 73(5–6): 51–65.
- [4] GUO Hua-jun, LIANG Ru-fu, LI Xin-hai, ZHANG Xin-ming, WANG Zhi-xing, PENG Wen-jie, WANG Zhao. Effect of calcination temperature on characteristics of  $\text{LiNi}_{1/3}\text{Co}_{1/3}\text{Mn}_{1/3}\text{O}_2$  cathode for lithium ion batteries [J]. *Transactions of Nonferrous Metals Society of China*, 2007, 17(6): 1307–1311.
- [5] HONG T E, JEONG E D, BAEK S R, BYEON M R, LEE Y S, KHAN F N, YANG H S. Nano SIMS characterization of boron- and aluminum-coated  $\text{LiNi}_{1/3}\text{Co}_{1/3}\text{Mn}_{1/3}\text{O}_2$  cathode materials for lithium secondary ion batteries [J]. *Journal of Applied Electrochemistry*, 2011, 42(1): 41–46.
- [6] LI Xiao-wei, LIN Ying-bin, LIN Ying, LAI Heng, HUANG Zhi-gao. Surface modification of  $\text{LiNi}_{1/3}\text{Co}_{1/3}\text{Mn}_{1/3}\text{O}_2$  with  $\text{Cr}_2\text{O}_3$  for lithium ion batteries [J]. *Rare Metals*, 2012, 31(2): 140–144.
- [7] SINGH G, THOMAS R, KUMAR A, KATIYAR R S, MANIVANNAN A. Electrochemical and structural investigations on ZnO treated  $0.5\text{Li}_2\text{MnO}_3\text{--}0.5\text{LiMn}_{0.5}\text{Ni}_{0.5}\text{O}_2$  layered composite cathode material for lithium ion battery [J]. *Journal of the Electrochemical Society*, 2012, 159(4): A470–A478.
- [8] KIM J H, PARK M S, SONG J H, BYUN D J, KIM Y J, KIM J S. Effect of aluminum fluoride coating on the electrochemical and thermal properties of  $0.5\text{Li}_2\text{MnO}_3\text{--}0.5\text{LiNi}_{0.5}\text{Co}_{0.2}\text{Mn}_{0.3}\text{O}_2$  composite material [J]. *Journal of Alloys and Compounds*, 2012, 517: 20–25.
- [9] WANG Hai-yan, TANG Ai-dong, HUANG Ke-long, LIU Su-qin. Uniform  $\text{AlF}_3$  thin layer to improve rate capability of  $\text{LiNi}_{1/3}\text{Co}_{1/3}\text{Mn}_{1/3}\text{O}_2$  material for Li-ion batteries [J]. *Transactions of Nonferrous Metals Society of China*, 2010, 20(5): 803–808.
- [10] YANG Kai, FAN Li-zhen, GUO Jia, QU Xuan-hui. Significant improvement of electrochemical properties of  $\text{AlF}_3$ -coated  $\text{LiNi}_{0.5}\text{Co}_{0.2}\text{Mn}_{0.3}\text{O}_2$  cathode materials [J]. *Electrochimica Acta*, 2012, 63: 363–368.
- [11] XU Ke, JIE Zhi-fu, LI Rong-hua, CHEN Zhi-xin, WU Shu-ting, GU Jia-fang, CHEN Jian-zhong. Synthesis and electrochemical properties of  $\text{CaF}_2$ -coated for long-cycling  $\text{Li}[\text{Mn}_{1/3}\text{Co}_{1/3}\text{Ni}_{1/3}]\text{O}_2$  cathode materials [J]. *Electrochimica Acta*, 2012, 60: 130–133.
- [12] BAI Yan-song, WANG Xian-you, YANG Shun-yi, ZHANG Xiao-yan, YANG Xiu-kang, SHU Hong-bo, WU Qiang. The effects of  $\text{FePO}_4$ -coating on high-voltage cycling stability and rate capability of  $\text{Li}[\text{Ni}_{0.5}\text{Co}_{0.2}\text{Mn}_{0.3}]\text{O}_2$  [J]. *Journal of Alloys and Compounds*, 2012, 541: 125–131.
- [13] SUN Y K, HAN J M, MYUNG S T, LEE S W, AMINE K. Significant improvement of high voltage cycling behavior  $\text{AlF}_3$ -coated  $\text{LiCoO}_2$  cathode [J]. *Electrochemistry Communications*, 2006, 8: 821–826.
- [14] LI Jian-gang, ZHANG Ya-yuan, LI Jian-jun, WANG Li, HE Xiang-ming, GAO Jian.  $\text{AlF}_3$  coating of  $\text{LiNi}_{0.5}\text{Mn}_{1.5}\text{O}_4$  for high-performance Li-ion batteries [J]. *Ionics*, 2011, 17: 671–675.
- [15] LEE S H, YOON C S, AMINE K, SUN Y K. Improvement of long-term cycling performance of  $\text{Li}[\text{Ni}_{0.8}\text{Co}_{0.15}\text{Al}_{0.05}]\text{O}_2$  by  $\text{AlF}_3$  coating [J]. *Journal of Power Sources*, 2013, 234: 201–207.
- [16] TANG Ai-dong, HUANG Ke-long. Electrochemical properties and structural characterization of layered  $\text{Li}_x\text{Ni}_{0.35}\text{Co}_{0.3}\text{Mn}_{0.35}\text{O}_{2+\delta}$  cathode materials [J]. *Mater Sci Eng B*, 2005, 122: 115–120.
- [17] SUN Y K, LEE M J, YOON C S, HASSOUN J, AMINE K, SCROSATI B. The role of  $\text{AlF}_3$  coatings in improving electrochemical cycling of Li-enriched nickel-manganese oxide electrodes for Li-ion batteries [J]. *Advanced Materials*, 2012, 24(9): 1192–1196.
- [18] LI J, KLOPSCH R, STAN M C, NOWAK S, KUNZE M, WINTER M, PASSERINI S. Synthesis and electrochemical performance of the high voltage cathode material  $\text{Li}[\text{Li}_{0.2}\text{Mn}_{0.56}\text{Ni}_{0.16}\text{Co}_{0.08}]\text{O}_2$  with improved rate capability [J]. *Journal of Power Sources*, 2011, 196(10): 4821–4825.
- [19] KANG S H, KEMPGENS P, GREENBAUM S, KROPF A J, AMINE K, THACKERAY M M. Interpreting the structural and electrochemical complexity of  $0.5\text{Li}_2\text{MnO}_3\text{--}0.5\text{LiMO}_2$  electrodes for lithium batteries ( $\text{M}=\text{Mn}_{0.5-x}\text{Ni}_{0.5-x}\text{Co}_{2x}$ ,  $0\leq x\leq 0.5$ ) [J]. *Journal of Materials Chemistry*, 2007, 17(20): 2069–2077.
- [20] MAHESH K C, MANJUNATHA H, VENKATESHA T V, SURESH G S. Study of lithium ion intercalation/de-intercalation into  $\text{LiNi}_{1/3}\text{Mn}_{1/3}\text{Co}_{1/3}\text{O}_2$  in aqueous solution using electrochemical impedance spectroscopy [J]. *Journal of Solid State Electrochemistry*, 2012, 16(9): 3011–3025.
- [21] LIM J H, BANG H, LEE K S, AMINE K, SUN Y K. Electrochemical characterization of  $\text{Li}_2\text{MnO}_3\text{--Li}[\text{Ni}_{1/3}\text{Co}_{1/3}\text{Mn}_{1/3}]\text{O}_2\text{--LiNiO}_2$  cathode synthesized via co-precipitation for lithium secondary batteries [J]. *Journal of Power Sources*, 2009, 189(1): 571–575.

- [22] ARUNKUMAR T A, WU Y, MANTHIRAM A. Factors influencing the irreversible oxygen loss and reversible capacity in layered  $\text{Li}[\text{Li}_{1/3}\text{Mn}_{2/3}]\text{O}_2\cdot\text{Li}[\text{M}]\text{O}_2$  ( $\text{M}=\text{Mn}_{0.5-y}\text{Ni}_{0.5-y}\text{Co}_{2y}$ , and  $\text{Ni}_{1-y}\text{Co}_y$ ) solid solutions [J]. Chemistry of Materials, 2007, 19: 3067–3073.
- [23] HONG J, LIM H D, LEE M, KIM S W, KIM H, OH S T, CHUNG G C, KANG K. Critical role of oxygen evolved from layered Li-excess metal oxides in lithium rechargeable batteries [J]. Chemistry of Materials, 2012, 24(14): 2692–2697.
- [24] JAFATA C J, OZOEMENA K I, MATHE M K, ROOS W D. Synthesis, characterisation and electrochemical intercalation kinetics of nanostructured aluminium-doped  $\text{Li}[\text{Li}_{0.2}\text{Mn}_{0.54}\text{Ni}_{0.13}\text{Co}_{0.13}]\text{O}_2$  cathode material for lithium ion battery [J]. Electrochimica Acta, 2012, 85: 411–422.
- [25] MTRTHA S K, NANDA J, VEITH G M, DUDNEY N J. Electrochemical and rate performance study of high-voltage lithium-rich composition:  $\text{Li}_{1.2}\text{Mn}_{0.525}\text{Ni}_{0.175}\text{Co}_{0.1}\text{O}_2$  [J]. Journal of Power Sources, 2012, 199: 220–226.
- [26] LIU Ling, SUN Ke-ning, ZHANG Nai-qing, YANG Tong-yong. Improvement of high-voltage cycling behavior of  $\text{Li}(\text{Ni}_{1/3}\text{Co}_{1/3}\text{Mn}_{1/3})\text{O}_2$  cathodes by Mg, Cr, and Al substitution [J]. Journal of Solid State Electrochemistry, 2008, 13(9): 1381–1386.

## $\text{AlF}_3$ 包覆锂离子电池正极材料 $\text{Li}_{1.2}(\text{Mn}_{0.54}\text{Ni}_{0.16}\text{Co}_{0.08})\text{O}_2$ 的制备、表征及电化学性能

李 艳, 刘开宇, 吕美玉, 魏 来, 钟剑剑

中南大学 化学化工学院, 长沙 410083

**摘 要:** 采用溶胶-凝胶法合成锂离子电池正极材料  $\text{Li}_{1.2}(\text{Mn}_{0.54}\text{Ni}_{0.16}\text{Co}_{0.08})\text{O}_2$ , 并用  $\text{AlF}_3$  对这种材料进行表面包覆改性。采用 X 射线衍射(XRD)、扫描电子显微镜(SEM)、高分辨率透射电子显微镜(HRTEM)等表征材料的结构和形貌。结果表明, 合成的  $\text{Li}_{1.2}(\text{Mn}_{0.54}\text{Ni}_{0.16}\text{Co}_{0.08})\text{O}_2$  具有典型的层状  $\alpha\text{-NaFeO}_2$  结构,  $\text{AlF}_3$  均匀包覆在  $\text{Li}_{1.2}(\text{Mn}_{0.54}\text{Ni}_{0.16}\text{Co}_{0.08})\text{O}_2$  材料表面, 包覆层厚度为 5~7 nm。电化学测试表明, 包覆  $\text{AlF}_3$  后材料的电化学性能得到提高, 在 1C 倍率下, 包覆的  $\text{AlF}_3$  材料的首次放电容量为 208.2 mA·h/g, 50 次循环后容量保持率为 72.4%, 而未包覆  $\text{AlF}_3$  的材料的首次放电容量和容量保持率分别为 191.7 mA·h/g 和 51.6%。

**关键词:** 锂离子电池;  $\text{Li}_{1.2}(\text{Mn}_{0.54}\text{Ni}_{0.16}\text{Co}_{0.08})\text{O}_2$ ;  $\text{AlF}_3$  表面包覆; 容量保持率

(Edited by Xiang-qun LI)